Available online at www.sciencedirect.com
SCIENCE DIRECT
ELSEVIER
Journal of the European Ceramic Society 26 (2006) 1845–1851
ECERS
www.elsevier.com/locate/jeurceramsoc

# Low-temperature microwave and THz dielectric response in novel microwave ceramics

S. Kamba [a,*], D. Noujni [a], A. Pashkin [a], J. Petzelt [a], R.C. Pullar [b], A.-K. Axelsson [b], N. McN Alford [b]

[a] *Institute of Physics, ASCR, Na Slovance 2, 182 21 Prague 8, Czech Republic*
[b] *London South Bank University, 103 Borough Road, London SE1 0AA, UK*

Available online 19 October 2005

**Abstract**

Low-temperature dielectric properties of $BaZn_{1/3}Nb_{2/3}O_3$-based ceramics, $CeO_2$-based ceramics and Ruddlesden–Popper $Sr_{n+1}Ti_nO_{3n+1}$ ($n = 1$–4) ceramics has been studied in microwave, THz and infrared frequency range down to 10 K. Extrinsic dielectric losses originating probably from diffusion of charged defects are observed in two families of compounds by a minimum in the temperature dependence of microwave quality $Q$. The rise of microwave permittivity and dielectric losses at low temperatures in $Sr_{n+1}Ti_nO_{3n+1}$ ($n = 2$–4) ceramics was explained by softening of an optical polar mode in $SrTiO_3$, which is in the $Sr_{n+1}Ti_nO_{3n+1}$ ($n = 3$, 4) ceramics contained as a second phase.


*Keywords:* Dielectric properties; Spectroscopy; Perovskites; Microwave ceramics

## 1. Introduction

Modern communication systems have moved to the microwave (MW) frequency region, where advanced dielectric ceramics are frequently used in resonators and filters. Miniaturization requires high relative permittivity ($\varepsilon'$) materials (since the size of resonators is inversely proportional to $\sqrt{\varepsilon'}$) with a small or zero temperature coefficient of resonance frequency $\tau_f$ ($|\tau_f| < 10\,\text{ppm}\,\text{K}^{-1}$). Furthermore, ceramics with low dielectric loss $\varepsilon''$ (often described in terms of high dielectric quality, $Q = \varepsilon'/\varepsilon''$) are needed for the high selectivity and optimized bandwidth of the filters. Within the last 20 years many new suitable ceramics with high $\varepsilon'$ and low $\tau_f$ were described. However, it was shown that although the two former parameters are not very dependent on the method of sample preparation, the quality $Q$ is extremely sensitive on conditions of sample preparation. It is not rare that in some cases the $Q$ value varies within 2 orders of magnitude depending on sintering temperature, cooling rate, atmosphere of annealing, etc. Technologists spent much time with improvement of sample processing to obtain losses as low as possible (highest $Q$), but the methods used were purely empirical, without knowing the lowest limit of the losses (intrinsic losses) with an origin in multi-phonon absorption.

Almost 20 years ago, Wakino et al.[1,2] proposed infrared (IR) reflectivity spectroscopy as a tool for investigating the intrinsic MW dielectric properties of dielectric resonators. It is well known that the main infrared dispersion of the permittivity is given by the sum of polar phonon contributions

$$\varepsilon^*(\omega) = \varepsilon'(\omega) - \mathrm{i}\omega''(\omega) = \sum_{j=1}^{n} \frac{\Delta\varepsilon_j \omega_j^2}{\omega_j^2 - \omega^2 + \mathrm{i}\omega\gamma_j} + \varepsilon_\infty \qquad (1)$$

where $\omega_j$ and $\gamma_j$ are the frequency and damping of the $j$th polar phonon, respectively; $\Delta\varepsilon_j$ denotes the mode contribution to the static permittivity $\varepsilon'(0)$ and $\varepsilon_\infty$ denotes the electronic part of the permittivity. We note that this formula is as a rule valid in dielectrics with $\varepsilon'(0) \leq 100$. In higher permittivity materials (e.g. ferroelectrics) an additional dispersion occurs below polar phonon frequencies, in the simplest case modelled by a Debye relaxation $\Delta\varepsilon_r\omega_r/(\omega_r + \mathrm{i}\omega)$ ($\Delta\varepsilon_r$ and $\omega_r$ are the dielectric strength and relaxation frequency, respectively), which should be added into Eq. (1).

Wakino et al.[1,2] mentioned that extrapolation of Eq. (1) from IR down to MW range, i.e. 2–3 orders of magnitude below $\omega_j$'s

* Corresponding author. Tel.: +420 2 6605 2957; fax: +420 2 8689 0527.
*E-mail address:* kamba@fzu.cz (S. Kamba).

0955-2219/$ – see front matter © 2005 Elsevier Ltd. All rights reserved.
doi:10.1016/j.jeurceramsoc.2005.09.010

gives constant real part of the permittivity

$$\varepsilon' = \varepsilon_\infty + \sum_{j=1}^{n} \Delta\varepsilon_j, \tag{2}$$

while the dielectric losses $\varepsilon''$ are proportional to frequency

$$\varepsilon''(\omega) \propto \omega \sum_{j=1}^{n} \frac{\Delta\varepsilon\gamma_j}{\omega_j^2}. \tag{3}$$

At high temperatures (around and above room temperature) the phonon damping should be linearly temperature dependent so that one can expect

$$\varepsilon''(\omega, T) \propto \omega \times T \tag{4}$$

This implies that the dielectric loss could be linearly extrapolated from the THz range (0.1–3 THz) down to the MW region. Later on it was shown[3,4] that for an accurate determination of the complex permittivity in the THz range it is more suitable to use the THz transmission spectroscopy than IR reflectivity, because it is much more sensitive to weak absorption effects. Simultaneously, it was shown that the extrinsic absorption mechanisms contribute only slightly to the THz and IR absorption, therefore, the linear extrapolation from THz to the MW range allows us to estimate predominantly the intrinsic dielectric losses stemming from the multi-phonon absorption.[3,4]

The method described above was used in the study of many MW ceramics[3,4] and it was shown that it gives rather good estimate of intrinsic MW losses, although the Eq. (1) is valid only in the range near phonon frequencies and the use of this formula is not theoretically justified for frequencies much lower than $\omega_j$, i.e. in MW range.

Gurevich and Tagantsev[5–7] developed a comprehensive microscopic phonon transport theory and have shown that depending on crystalline symmetry, temperature interval, frequency range and some parameters of the phonon spectrum, the temperature and frequency dependence of intrinsic dielectric loss can be described by a power law.[6]

$$\varepsilon''(\omega, T) \approx \omega^n \times T^m \tag{5}$$

where $n = 1$–5 and $m = 1$–9. In the MW range, far below the frequencies of mean phonon damping, two-phonon difference decay processes dominate at room and medium–high temperatures and the theory predicts

$$\varepsilon''(\omega, T) \approx \omega \times T^2. \tag{6}$$

Both approaches, the damped oscillator model as well as microscopic phonon transport theory, give in some limited cases, the linear frequency dependence of $\varepsilon''(\omega)$, but the temperature dependence in Eq. (4) is not the same (it agrees only for crystals of symmetry 4/*m* and 6/*m*).[7] We note that at low temperatures Eq. (6) is not valid and more general Eq. (5) with steeper temperature dependences is theoretically expected.

As was already mentioned, the total MW dielectric loss consists of intrinsic and extrinsic contributions. Extrinsic losses are caused by lattice defects and therefore can be in principle removed by proper material processing. Various types of defects can play a role: point defects (isotopes, dopant atoms, vacancies, defect pairs, positional disorder in complex systems), linear defects (dislocations), planar defects (grain boundaries, domain walls) and volume defects (pores, inclusions, secondary phases).[8] Depending on the kind of defects, frequency and temperature dependence of extrinsic losses can be different.

(1) *Defect induced one-phonon absorption*: In the case of static disorder the momentum conservation is relaxed due to breaking of the translation symmetry and a linear part of the acoustic branches activates in the MW and THz spectra. As long as the concentration of defects is temperature independent, the losses are also temperature independent. The microscopic calculations yield[6] $\varepsilon''(\omega) \propto \omega$ for uncorrelated charged point defects and uncharged planar defects; $\varepsilon''(\omega) \propto \omega^2$ for uncharged linear defects and $\varepsilon''(\omega) \propto \omega^3$ for uncharged point defects. In the case of correlated charged point defects $\varepsilon''(\omega) \propto \omega^3$ up to the frequency $\omega_c \approx v/\xi$ where $v$ is the mean transverse acoustic velocity and $\xi$ the correlation length.[9] Realistic estimates give 1–10 nm so that $\omega_c \approx 10^{10}$–$10^{12}$ Hz.

(2) *Phonon scattering on defects*: This reduces the phonon lifetime, i.e. increases the phonon damping (independent of *T*). The main effect on the loss spectrum concerns the enhanced damping of polar phonon modes, which enhances also the THz and extrapolated MW losses.

(3) *Absorption associated with localized defect vibrations*: This may influence the THz losses in the case of heavy or weakly bound defects which give rise to so called resonant modes (local defect modes coupled with acoustic vibrations).[10] Their direct influence on MW losses is probably negligible, but a two-resonant-phonon absorption can give rise to a quasi-Debye[6] type absorption in the case when the defect environment lacks inversion symmetry.

(4) *Losses connected directly with strongly anharmonic motion (diffusion) of charged defects*: As a rule, such a motion gives rise to broad relaxation-like loss maxima with thermally activated relaxation frequencies and strengths. Such relaxation was observed for example in $LaAlO_3$ single crystals.[11] In weakly disordered dielectrics these effects dominate mostly below the MW range, but no systematic experimental studies are available because an extremely broad frequency and temperature range should be covered to elucidate the corresponding loss mechanism.

It is the aim of this short paper to review temperature dependences of MW and THz dielectric response in various MW ceramics down to 20 K and try to show how one can distinguish the intrinsic and extrinsic dielectric losses from the spectra.

## 2. $BaZn_{1/3}Nb_{2/3}O_3$-based ceramics

$BaZn_{1/3}Ta_{2/3}O_3$ ceramics are popular as resonators in mobile telephone base station filters because of their excellent dielectric properties ($\varepsilon' = 30$, $Q \times f = 150$ THz, $\tau_f = 1$ ppm $K^{-1}$). However, there is a long-term effort to replace expensive Ta-containing compounds by much cheaper Nb analogues. $BaZn_{1/3}Nb_{2/3}O_3$

has $\varepsilon' = 38$, $Q \times f = 90$ THz but an unacceptably high $\tau_f$ of 30 ppm $K^{-1}$,[12] which makes direct application of these ceramics in MW devices impossible. Hughes et al.[13] achieved $\tau_f = 0$ in $0.9Ba[(Zn_{0.6}Co_{0.4})_{1/3}Nb_{2/3}]O_3$–$0.1Ba(Ga_{0.5}Ta_{0.5})O_3$ ceramics, Ahn et al.[14,15] and independently Scott et al.[16] removed expensive Ta completely and obtained excellent dielectric properties with $\tau_f = 0$ in $(1-x)Ba(Co_{1/3}Nb_{2/3}O_3)O_3$–$xBa(Zn_{1/3}Nb_{2/3})O_3$ for $x = 0.3$ and 0.4, respectively. In all the cases $\varepsilon'$ and quality $Q$ remained sufficiently high.

We have investigated MW, THz and lattice dynamics properties of $(1-x)Ba(Zn_{1/3}Nb_{2/3})O_3$–$xBa(Ga_{0.5}Ta_{0.5})O_3$ (BZN–$x$BGT) for $x$ between 0 and 0.2 as well as $0.9Ba[(Zn_{0.6}Co_{0.4})_{1/3}Nb_{2/3}]O_3$–$0.1Ba(Ga_{0.5}Ta_{0.5})O_3$ (i.e. BZCN–0.1BGT) ceramics. THz and MW measurements have been performed at temperatures down to 10 K and the detailed results and measurement techniques were described in Ref.[17] It was shown that $\tau_f$ reduces with increasing BGT content and BZCN–0.1BGT could reach zero $\tau_f$ while $\varepsilon'$ is only slightly influenced by BGT content and remains above 31 in all samples.

Fig. 1 shows the temperature dependence of the MW quality factor $Q$ at approximately 3 GHz. The actual resonance frequencies vary slightly, depending on the sample and temperature. The significant temperature dependence of $Q$ is controlled mainly by $\varepsilon''(T)$ because $\varepsilon'$ is only slightly temperature dependent. As mentioned above, two-phonon difference decay processes dominate at room and medium–high temperatures and in this case the microscopic phonon transport theory predicts that the intrinsic MW losses will be proportional to temperature squared (see Eq. (6)). At low temperatures even steeper temperature dependence can be expected. The squared temperature dependence is plotted also in the Fig. 1 and it is seen that no sample follows such temperature dependence. Non-monotonous temperature dependences of $Q(T)$ with minima near 150 and below 50 K are seen in most samples, which are caused obviously by extrinsic loss contributions. The minima in $Q(T)$ are due to dielectric relaxations which slow down on cooling (usually according to the Arrhenius law if the relaxation is due to a thermally activated process) and cross the measuring resonance frequency of ~3 GHz at two different temperatures. We speculate that the diffusions of charged defects are responsible for the relaxations, because $(1-x)Ba(Zn^{2+}_{1/3}Nb^{5+}_{2/3})O_3 - xBa(Ga^{3+}_{0.5}Ta^{5+}_{0.5})O_3$ contains four different types of ions at B sites with three different valences. An inhomogeneous distribution of $Zn^{2+}$, $Nb^{5+}$, $Ga^{3+}$ and $Ta^{5+}$ at B sites causes random fields and thus charged defects, which may be the origin of the dielectric relaxations.

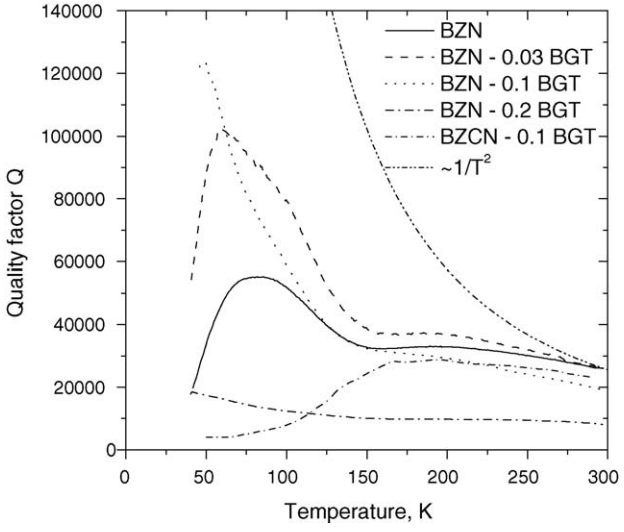


Fig. 1. Temperature dependence of the MW quality factor ($Q$) of BZN–$x$BGT and BZCN–0.1BGT ceramics at ~3 GHz (after Ref.[17]).

The room temperature $\varepsilon'(\omega)$ and $\varepsilon''(\omega)$ spectra obtained from the fit of IR reflectivity and extrapolated down to MW range are plotted together with experimental MW and THz data in Fig. 2. The IR reflectivity is sensitive only to strong absorption mechanisms, which in our case are intrinsic absorption processes dominated by one-phonon absorption. Time-domain THz transmission spectroscopy is more sensitive and can therefore also resolve weak extrinsic absorption processes. For this reason the $\varepsilon''(\omega)$ spectra obtained from the fit of IR reflectivity spectra do not correspond very well to THz and MW experimental data (Fig. 2b), where distinct extrinsic contributions exist. Conversely, there is a very good correspondence between the MW and THz $\varepsilon'$ data (Fig. 2a), which shows that the extrinsic absorption is rather low and does not contribute to the real part of permittivity appreciably. It seems that the highest extrinsic contribution to $\varepsilon''(\omega)$ is in BZN–0.2BGT ceramics, i.e. in the sample with the highest concentration of charged defects. This idea is supported not only by Fig. 2b, but also by Fig. 1, where only small temperature dependence of $Q$ is seen. It gives evidence that the extrinsic losses dominate in BZN–0.2BGT ceramics and probably static-disorder induced one-phonon absorption plays the role here. BZCN–0.1BGT shows a very good correspondence between IR, THz and MW data, which supports the idea that the Co ions compensate partially the charge point defects and reduce the extrinsic losses. Nevertheless, the strong drop of $Q$ below 150 K gives also evidence about the temperature dependent extrinsic losses in this ceramics.

## 3. $CeO_2$-based MW ceramics

$CeO_2$ ceramics were mostly studied from the point of view of ionic conductivity since $CeO_2$ doped with various dopants (e.g. $Y_2O_3$) shows excellent ionic conductivity at high temperatures.[18] Nevertheless, at room temperatures it is a good dielectric with $\varepsilon' = 23$, $Q \times f = 60$ THz, but rather high $\tau_f = -53$ ppm $K^{-1}$. We tried to reduce $\tau_f$ by addition of $CaCO_3$ or $TiO_2$ and really observed that $\tau_f$ reduced to $-33$ ppm $K^{-1}$ in $CeO_2$ with 4.3% of $TiO_2$.[19] However, the $Q \times f$ factor also noticeably dropped down to 10 THz. In the case of $CeO_2$–$xCaCO_3$ with $x = 1\%$ a remarkable increase of $Q \times f$ to 120 THz was observed, but $\tau_f$ was even worse than in pure $CeO_2$ and both $\tau_f$ and $Q$ deteriorated with increasing concentration of $CaCO_3$. In Fig. 3 we compared the temperature dependences of $Q \times f$ in pure $CeO_2$ ceramics with the best doped samples $CeO_2$–1% $TiO_2$ and $CeO_2$–1% $CaCO_3$. In all samples $Q \times f$ increases at low temperatures due to the reduced intrinsic losses. Nevertheless, the influence of extrinsic losses is also seen. A broad minimum appears in pure $CeO_2$ near 100 K, probably due to slowing down of a relaxation originating probably from diffusion of

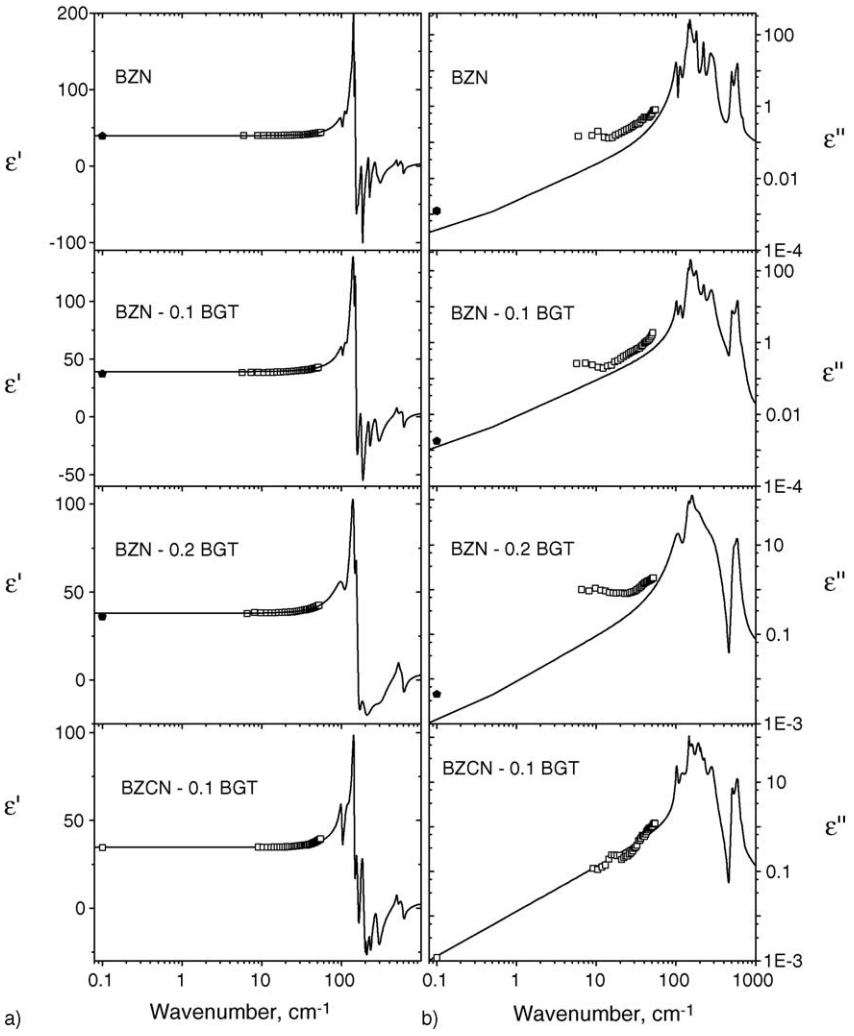


Fig. 2. Room-temperature relative permittivity (a) and dielectric loss spectra (b) obtained from the fits of IR and THz spectra. Points are experimental MW and THz data (after Ref.[17]).

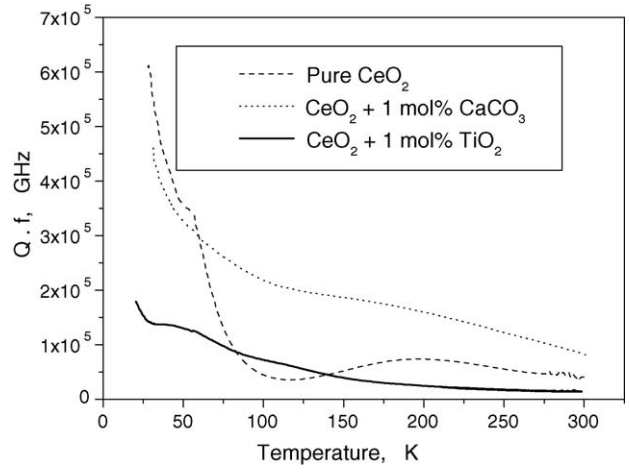


Fig. 3. Temperature dependence of $Q \times f$ in pure and doped $CeO_2$. Resonance frequencies were ~5.5 GHz (after Ref.[19]).

some oxygen vacancies. Below 80 K, the extrinsic relaxation drops below the resonance frequency 5.5 GHz. This means that the extrinsic contribution does not contribute anymore to the losses at lower temperatures and because the intrinsic losses also steeply reduce on cooling (Eq. (5)), $Q \times f$ strongly increases on cooling, as seen in Fig. 3. In $CeO_2$–1% $CaCO_3$ ceramics, a smaller influence of the extrinsic relaxation is seen (shallow minimum above 100 K), therefore the $Q \times f$ is higher than in pure $CeO_2$ at almost all temperatures. A small amount of $CaCO_3$ probably reduces the oxygen vacancy concentration. In the case of $CeO_2$–1% $TiO_3$, the $Q \times f$ is lower than in the previous two samples giving evidence for higher losses. They remain high also at low temperatures so that the origin of extrinsic losses is probably different than in the previous samples.

## 4. Ruddlesden–Popper $Sr_{n+1}Ti_nO_{3n+1}$ ceramics ($n = 1$–4)

$Sr_{n+1}Ti_nO_{3n+1}$ belong to the class of Ruddlesden–Popper compounds, composed of $n$ perovskite blocks of $SrTiO_3$

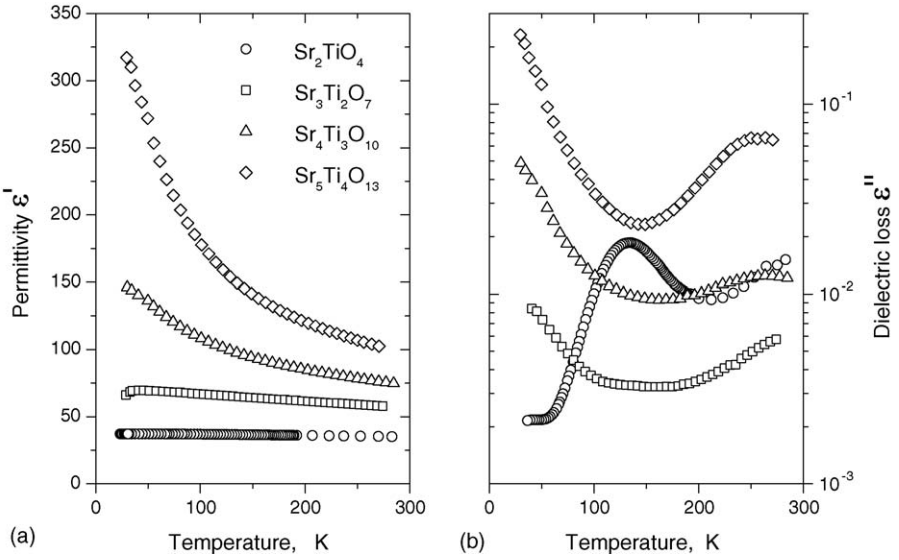


Fig. 4. Temperature dependence of MW permittivity (a) and dielectric loss (b) of $Sr_{n+1}Ti_nO_{3n+1}$ ($n = 1$–4) ceramics (after Ref.[24]).

oriented along the [0 0 1] direction, separated by rock-salt type SrO layers.[20] The number of perovskite layers controls the value of room temperature permittivity $\varepsilon'$ of the system; the higher number of perovskite layers the higher permittivity, but unfortunately also the higher $\tau_f$. $Sr_2TiO_4$ has $\varepsilon' = 37$ ($\tau_f = 137\,ppm\,K^{-1}$), $Sr_5Ti_4O_{13}$ shows $\varepsilon' = 100$ ($\tau_f = 801\,ppm\,K^{-1}$), and the end member ($n = \infty$) of the series, $SrTiO_3$, exhibits $\varepsilon' = 290$ ($\tau_f = 1647\,ppm\,K^{-1}$).[21,22], $Q$ does not behave in such a monotonous way and the highest $Q$ was observed in $Sr_3Ti_2O_7$ ($Q \times f = 19$ THz).[21] We investigated $Sr_{n+1}Ti_nO_{3n+1}$ ceramics with $n = 1$–4 and pure $SrTiO_3$ ($n = \infty$). On the basis of the room temperature IR reflectivity and THz transmission spectra we suggested that the explanation of the dielectric behaviour in this system was by softening of the lowest frequency polar phonon with the increasing number of perovskite layers.[23] For confirmation of this idea we performed dielectric MW, THz and IR reflectivity measurements down to 10 K.[24] Fig. 4 shows the temperature dependences of $\varepsilon'$ and $\varepsilon''$ in $Sr_{n+1}Ti_nO_{3n+1}$ measured at frequencies near 3 GHz. Two characteristic features are seen: (1) magnitude of $\varepsilon'$ and its temperature dependence increases with $n$; the samples with $n = 3$ and 4 exhibit temperature behaviour of $\varepsilon'$ similar to the incipient ferroelectric $SrTiO_3$, only the values of $\varepsilon'$ are much lower than in $SrTiO_3$. (2) $\varepsilon''$ shows a non-monotonous behaviour which will be discussed below.

FTIR reflectivity and THz spectra exhibited small temperature dependences for samples with $n = 1$ and 2 (see Fig. 5a), yielding small changes in extrapolated MW $\varepsilon'(T)$. Samples with $n = 3$ and 4 showed remarkable changes predominantly in the frequency range below 100 $cm^{-1}$ (see Fig. 5b) due to the phonon mode softening (see Fig. 5b). FTIR reflectivity spectra were fitted together with THz spectra with a generalized four-parameter damped oscillator model.[23] Examples of the resulting $\varepsilon'(\omega)$ and $\varepsilon''(\omega)$ spectra of $Sr_5Ti_4O_{13}$, including MW and THz data are shown in Fig. 6. One can see that the MW $\varepsilon'(T)$ is completely described by the polar phonon contribution and its increase upon cooling is the consequence of phonon softening. Temperature dependence of the soft mode (SM) frequency in $Sr_{n+1}Ti_nO_{3n+1}$

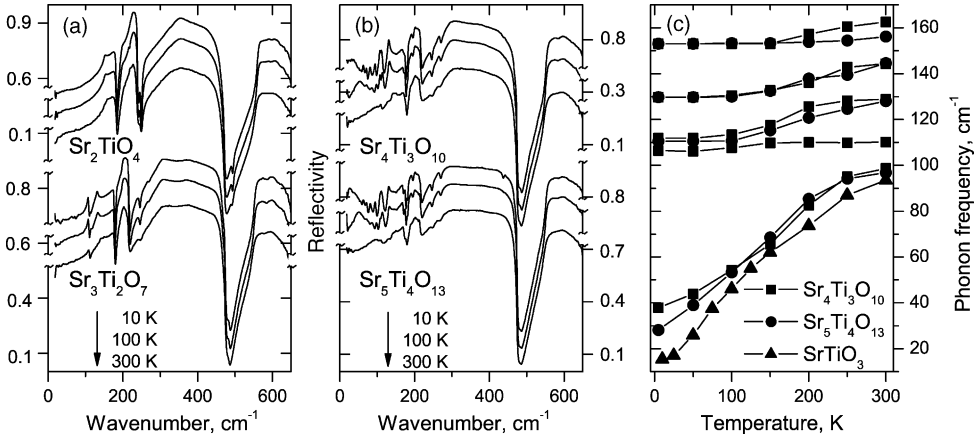


Fig. 5. (a) IR reflectivity spectra of $Sr_2TiO_4$ and $Sr_3Ti_2O_7$ and (b) $Sr_4Ti_3O_{10}$ and $Sr_5Ti_4O_{13}$ at various temperatures. (b) Temperature dependence of the lowest four phonon-mode frequencies in $Sr_{n+1}Ti_nO_{3n+1}$ ($n = 3, 4, \infty$). The data for $SrTiO_3$ were taken from Ref.[25].

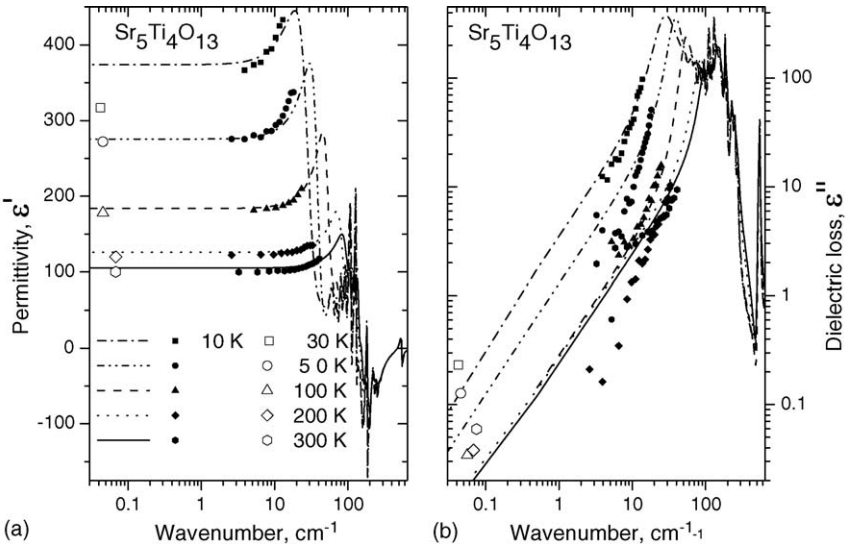


Fig. 6. Permittivity (a) and dielectric loss (b) spectra of $Sr_5Ti_4O_{13}$ at various temperatures calculated from the fits to the IR reflection and THz spectra. Experimental MW and THz data are marked with open and full dots, respectively.

($n = 3, 4, \infty$) is shown in Fig. 5b and one can see that it is very similar in all three samples. Only the dielectric strength of the SM increases with n and therefore the static $\varepsilon(0)$ increases up to $\varepsilon(0) \approx 10^3$–$10^4$ in $SrTiO_3$ at low temperatures.[25] One can speculate that the increase in the number of perovskite layers in the samples leads to the rise of the strength of the SM. However, XRD and TEM studies[21,22] of our samples revealed presence of $SrTiO_3$ (i.e. $n = \infty$) inclusions in the samples with $n = 3$ and 4. $Sr_4Ti_3O_{10}$ contains 10–20% of $n = \infty$ phase whereas $Sr_5Ti_4O_{13}$ comprises approximately twice that amount. Therefore, it might be that the SM originates predominantly from microscopic inclusions of the $n = \infty$ phase, implying that we are in fact measuring the effective dielectric response of a composite.

Let us comment on the temperature dependence of MW dielectric losses $\varepsilon''$ in Fig. 4b. A maximum in $\varepsilon''(T)$ near 140 K appears for the $n = 1$ sample due to a weak extrinsic (defect) relaxation. In the other three samples, the low-temperature rise in $\varepsilon''(T)$ (decrease in $Q$) has predominantly a phonon origin in SM softening. However, the SM comes from $SrTiO_3$ second phase.

## 5. Conclusion

The influence of extrinsic dielectric losses on the temperature dependence of the MW quality $Q$ has been demonstrated for $BaZn_{1/3}Nb_{2/3}O_3$ and $CeO_2$-based MW ceramics. The extrinsic dielectric relaxation, originating probably from diffusion of charged defects, gives small contribution to static permittivity, but has significant influence on the dielectric losses. On the other hand, it is shown that not always the increase in MW $\varepsilon''$ (i.e. decrease in $Q$) on cooling has its origin in diffusion of charged defects. $Sr_{n+1}Ti_nO_{3n+1}$ ceramics with $n = 2$–4 exhibit increase in both MW $\varepsilon'$ and $\varepsilon''$ on cooling due to softening of the optical soft phonon mode originating from $SrTiO_3$ second phase.

## Acknowledgments

We appreciate the support of the Grant Agency of the Czech Republic (project no. 202/04/0993), Czech Academy of Sciences (project no. A1010213) and Czech Ministry of Education (project COST OC 525.20).

## References

1. Wakino, K., Murata, M. and Tamura, H., Far-infrared reflection spectra of $Ba(ZnTa)O_3$–$BaZrO_3$ dielectric resonator material. *J. Am. Ceram. Soc.*, 1986, **69**, 34–37.
2. Tamura, H., Sagala, D. A. and Wakino, K., Lattice vibration of $Ba(ZnTa)O_3$ crystal with ordered perovskite structure. *Jpn. J. Appl. Phys.*, 1986, **25**(6), 787–791.
3. Petzelt, J., Kamba, S., Kozlov, G. V. and Volkov, A. A., Dielectric properties of microwave ceramics investigated by infrared and submillimetre spectroscopy. *Ferroelectrics*, 1996, **176**, 145–165.
4. Petzelt, J. and Kamba, S., Submillimetre and infrared response of microwave materials: extrapolation to microwave properties. *Mater. Chem. Phys.*, 2003, **79**, 175–180.
5. Gurevich, V. L., *Transport in Phonon Systems*. North Holland, Amsterdam, 1986.
6. Gurevich, V. L. and Tagantsev, A. K., *Adv. Phys.*, 1991, **40**, 719.
7. Tagansev, A. K., Sherman, V. O., Astafiev, K. F., Venkatesh, J. and Setter, N., Ferroelectric materials for microwave tunable applications. *J. Electroceram.*, 2003, **11**, 5–66.
8. Petzelt, J. and Setter, N., Far infrared spectroscopy and origin of microwave losses in low-loss ceramics. *Ferroelectrics*, 1993, **150**, 89–102.
9. Schlömann, E., Dielectric losses in ionic crystals with disordered charge distributions. *Phys. Rev.*, 1964, **135**, A413–A419.
10. Barker Jr., A. S. and Sievers, A. J., Optical studies of the vibrational properties of disordered solids. *Rev. Mod. Phys.*, 1975, **47**, S1–S179.
11. Zuccaro, C., Winter, M., Klein, N. and Urban, K., Microwave absorption in single crystals of lanthanum aluminate. *J. Appl. Phys.*, 1997, **82**, 5695–5704.
12. Nomura, S., Ceramics for microwave dielectric resonators. *Ferroelectrics*, 1983, **49**, 61–70.

13. Hughes, H., Iddles, D. M. and Reaney, I. M., Niobate-based microwave dielectrics suitable for third generation mobile phone base stations. *Appl. Phys. Lett.*, 2001, **79**, 2952–2954.
14. Ahn Ch.-W, Jang, H.-J., Nahm, S., Park, H.-M. and Lee, H.-J., Effects of microstructure on the microwave dielectric properties of $Ba(Co_{1/3}Nb_{2/3})O_3$ and $(1-x)Ba(Co_{1/3}Nb_{2/3})O_3$–$xBa(Zn_{1/3}Nb_{2/3})O_3$ ceramics. *J. Eur. Ceram. Soc.*, 2003, **23**, 2473–2478.
15. Ahn, Ch.-W., Hahm, S., Yoon, S.-J., Park, H.-M. and Lee, H.-J., Microstructure and microwave dielectric properties of $(1-x)Ba(Co_{1/3}Nb_{2/3})O_3$–$xBa(Zn_{1/3}Nb_{2/3})O_3$ ceramics. *Jpn. J. Appl. Phys.*, 2003, **42**, 6964–6968.
16. Scott, R. I., Thomas, M. and Hampson, C., Development of low cost, high performance $Ba(Zn_{1/3}Nb_{2/3})O_3$ based materials for microwave resonator applications. *J. Eur. Ceram. Soc.*, 2003, **23**, 2467–2471.
17. Kamba, S., Hughes, H., Noujni, D., Santhi, S., Pullar, R. C., Samoukhina, P. *et al.*, Relation between microwave and lattice vibration properties in $Ba(Zn_{1/3}Nb_{2/3})O_3$-based microwave dielectric ceramics. *J. Phys. D: Appl. Phys.*, 2004, **37**, 1980–1986.
18. Tian, C. and Chan, S. W., Ionic conductivities, sintering temperatures, and microstructures of bulk ceramic $CeO_2$ doped with $Y_2O_3$. *Solid State Ionics*, 2000, **134**, 89–102.
19. Santha, N. I., Sebastian, M. T., Mohanan, P., McN Alford, N., Sarma, K., Pullar, R. C. *et al.*, Effect of doping on the dielectric properties of cerium oxide in the microwave and far-infrared frequency range. *J. Am. Ceram. Soc.*, 2004, **87**, 1233–1237.
20. Tian, W., Pan, X. Q., Haeni, J. H. and Schlom, D. G., Transmission electron microscopy study of $n=1$–5 $Sr_{n+1}Ti_nO_{3n+1}$ epitaxial thin film. *J. Mater. Res.*, 2001, **16**, 2013–2026.
21. Wise, P. L., Reaney, I. M., Lee, W. E., Price, T. J., Iddles, D. M. and Cannel, D. S., Structure–microwave property relations in $(Sr_xCa_{(1-x)})_{n+1}Ti_nO_{3n+1}$. *J. Eur. Ceram. Soc.*, 2001, **21**, 1723–1726.
22. Wise, P. L., Reaney, I. M., Lee, W. E., Price, T. J., Iddles, D. M. and Cannel, D. S., Structure–microwave property relations of Ca and Sr titanates. *J. Eur. Ceram. Soc.*, 2001, **21**, 2629–2632.
23. Kamba, S., Samoukhina, P., Kadlec, F., Pokorný, J., Petzelt, J., Reaney, I. M. *et al.*, Composition dependence of the lattice vibrations in $Sr_{n+1}Ti_nO_{3n+1}$ Ruddlesden–Popper homologous series. *J. Eur. Ceram. Soc.*, 2003, **23**, 2639–2645.
24. Noujni, D., Kamba, S., Pashkin, A., Bovtun, V., Petzelt, J., Axelsson, A.-K. *et al.*, *Integr. Ferroelectr.*, 2004, **62**, 199–203.
25. Petzelt, J., Ostapchuk, T., Gregora, I., Rychetský, I., Hoffmann-Eifert, S., Pronin, A. V. *et al.*, Dielectric, infrared, and Raman response of undoped $SrTiO_3$ ceramics: evidence of polar grain boundaries. *Phys. Rev. B*, 2001, **64**, 184111/1–184111/10.